



Contents lists available at ScienceDirect

## Physics Letters B

www.elsevier.com/locate/physletb



## Energy and system size dependence of $\phi$ meson production in Cu + Cu and Au + Au collisions

STAR Collaboration

B.I. Abelev<sup>i</sup>, M.M. Aggarwal<sup>ae</sup>, Z. Ahammed<sup>au</sup>, B.D. Anderson<sup>s</sup>, D. Arkhipkin<sup>m</sup>, G.S. Averichev<sup>l</sup>, Y. Bai<sup>ab</sup>, J. Balewski<sup>w</sup>, O. Barannikova<sup>i</sup>, L.S. Barnby<sup>b</sup>, J. Baudot<sup>q</sup>, S. Baumgart<sup>az</sup>, D.R. Beavis<sup>c</sup>, R. Bellwied<sup>ax</sup>, F. Benedosso<sup>ab</sup>, M.J. Betancourt<sup>w</sup>, R.R. Betts<sup>i</sup>, S. Bharadwaj<sup>aj</sup>, A. Bhasin<sup>r</sup>, A.K. Bhati<sup>ae</sup>, H. Bichsel<sup>aw</sup>, J. Bielcik<sup>k</sup>, J. Bielcikova<sup>k</sup>, B. Biritz<sup>f</sup>, L.C. Bland<sup>c</sup>, M. Bombara<sup>b</sup>, B.E. Bonner<sup>ak</sup>, M. Botje<sup>ab</sup>, J. Bouchet<sup>s</sup>, E. Braidot<sup>ab</sup>, A.V. Brandin<sup>z</sup>, E. Bruna<sup>az</sup>, S. Bueltmann<sup>ad</sup>, T.P. Burton<sup>b</sup>, M. Bystersky<sup>k</sup>, X.Z. Cai<sup>an</sup>, H. Caines<sup>az</sup>, M. Calderón de la Barca Sánchez<sup>e</sup>, J. Callner<sup>i</sup>, O. Catu<sup>az</sup>, D. Cebra<sup>e</sup>, R. Cendejas<sup>f</sup>, M.C. Cervantes<sup>ap</sup>, Z. Chajecski<sup>ac</sup>, P. Chaloupka<sup>k</sup>, S. Chattopadhyay<sup>au</sup>, H.F. Chen<sup>am</sup>, J.H. Chen<sup>an</sup>, J.Y. Chen<sup>ay</sup>, J. Cheng<sup>ar</sup>, M. Cherney<sup>j</sup>, A. Chikanian<sup>az</sup>, K.E. Choi<sup>ai</sup>, W. Christie<sup>c</sup>, S.U. Chung<sup>c</sup>, R.F. Clarke<sup>ap</sup>, M.J. Coddington<sup>ap</sup>, J.P. Coffin<sup>q</sup>, R. Corliss<sup>w</sup>, T.M. Cormier<sup>ax</sup>, M.R. Cosentino<sup>al</sup>, J.G. Cramer<sup>aw</sup>, H.J. Crawford<sup>d</sup>, D. Das<sup>e</sup>, S. Dash<sup>n</sup>, M. Daugherty<sup>aq</sup>, C. De Silva<sup>ax</sup>, T.G. Dedovich<sup>l</sup>, M. DePhillips<sup>c</sup>, A.A. Derevschikov<sup>ag</sup>, R. Derradi de Souza<sup>g</sup>, L. Didenko<sup>c</sup>, P. Djawotho<sup>p</sup>, S.M. Dogra<sup>r</sup>, X. Dong<sup>v</sup>, J.L. Drachenberg<sup>ap</sup>, J.E. Draper<sup>e</sup>, F. Du<sup>az</sup>, J.C. Dunlop<sup>c</sup>, M.R. Dutta Mazumdar<sup>au</sup>, W.R. Edwards<sup>v</sup>, L.G. Efimov<sup>l</sup>, E. Elhalhuli<sup>b</sup>, M. Elnimr<sup>ax</sup>, V. Emelianov<sup>z</sup>, J. Engelage<sup>d</sup>, G. Eppley<sup>ak</sup>, B. Erazmus<sup>ao</sup>, M. Estienne<sup>q</sup>, L. Eun<sup>af</sup>, P. Fachini<sup>c</sup>, R. Fatemi<sup>t</sup>, J. Fedorisin<sup>l</sup>, A. Feng<sup>ay</sup>, P. Filip<sup>m</sup>, E. Finch<sup>az</sup>, V. Fine<sup>c</sup>, Y. Fisyak<sup>c</sup>, C.A. Gagliardi<sup>ap</sup>, L. Gaillard<sup>b</sup>, D.R. Gangadharan<sup>f</sup>, M.S. Ganti<sup>au</sup>, E. Garcia-Solis<sup>i</sup>, V. Ghazikhanian<sup>f</sup>, P. Ghosh<sup>au</sup>, Y.N. Gorbunov<sup>j</sup>, A. Gordon<sup>c</sup>, O. Grebenyuk<sup>v</sup>, D. Grosnick<sup>at</sup>, B. Grube<sup>ai</sup>, S.M. Guertin<sup>f</sup>, K.S.F.F. Guimaraes<sup>al</sup>, A. Gupta<sup>r</sup>, N. Gupta<sup>r</sup>, W. Guryn<sup>c</sup>, B. Haag<sup>e</sup>, T.J. Hallman<sup>c</sup>, A. Hamed<sup>ap</sup>, J.W. Harris<sup>az</sup>, W. He<sup>p</sup>, M. Heinz<sup>az</sup>, S. Heppelmann<sup>af</sup>, B. Hippolyte<sup>q</sup>, A. Hirsch<sup>ah</sup>, E. Hjort<sup>v</sup>, A.M. Hoffman<sup>w</sup>, G.W. Hoffmann<sup>aq</sup>, D.J. Hofman<sup>i</sup>, R.S. Hollis<sup>i</sup>, H.Z. Huang<sup>f</sup>, T.J. Humanic<sup>ac</sup>, G. Igo<sup>f</sup>, A. Iordanova<sup>i</sup>, P. Jacobs<sup>v</sup>, W.W. Jacobs<sup>p</sup>, P. Jakl<sup>k</sup>, F. Jin<sup>an</sup>, C.L. Jones<sup>w</sup>, P.G. Jones<sup>b</sup>, J. Joseph<sup>s</sup>, E.G. Judd<sup>d</sup>, S. Kabana<sup>ao</sup>, K. Kajimoto<sup>aq</sup>, K. Kang<sup>ar</sup>, J. Kapitan<sup>k</sup>, M. Kaplan<sup>h</sup>, D. Keane<sup>s</sup>, A. Kechechyan<sup>l</sup>, D. Kettler<sup>aw</sup>, V.Yu. Khodyrev<sup>ag</sup>, D.P. Kikola<sup>v</sup>, J. Kiryluk<sup>v</sup>, A. Kisiel<sup>ac</sup>, S.R. Klein<sup>v</sup>, A.G. Knospe<sup>az</sup>, A. Kocoloski<sup>w</sup>, D.D. Koetke<sup>at</sup>, M. Kopytine<sup>s</sup>, L. Kotchenda<sup>z</sup>, V. Kouchpil<sup>k</sup>, P. Kravtsov<sup>z</sup>, V.I. Kravtsov<sup>ag</sup>, K. Krueger<sup>a</sup>, M. Krus<sup>k</sup>, C. Kuhn<sup>q</sup>, L. Kumar<sup>ae</sup>, P. Kurnadi<sup>f</sup>, M.A.C. Lamont<sup>c</sup>, J.M. Landgraf<sup>c</sup>, S. LaPointe<sup>ax</sup>, J. Lauret<sup>c</sup>, A. Lebedev<sup>c</sup>, R. Lednicky<sup>m</sup>, C.-H. Lee<sup>ai</sup>, W. Leight<sup>w</sup>, M.J. LeVine<sup>c</sup>, C. Li<sup>am</sup>, Y. Li<sup>ar</sup>, G. Lin<sup>az</sup>, X. Lin<sup>ay</sup>, S.J. Lindenbaum<sup>aa</sup>, M.A. Lisa<sup>ac</sup>, F. Liu<sup>ay</sup>, H. Liu<sup>e</sup>, J. Liu<sup>ak</sup>, L. Liu<sup>ay</sup>, T. Ljubicic<sup>c</sup>, W.J. Llope<sup>ak</sup>, R.S. Longacre<sup>c</sup>, W.A. Love<sup>c</sup>, Y. Lu<sup>ay</sup>, T. Ludlam<sup>c</sup>, D. Lynn<sup>c</sup>, G.L. Ma<sup>an</sup>, Y.G. Ma<sup>an</sup>, D.P. Mahapatra<sup>n</sup>, R. Majka<sup>az</sup>, O.I. Mall<sup>e</sup>, L.K. Mangotra<sup>r</sup>, R. Manweiler<sup>at</sup>, S. Margetis<sup>s</sup>, C. Markert<sup>aq</sup>, H.S. Matis<sup>v</sup>, Yu.A. Matulenko<sup>ag</sup>, T.S. McShane<sup>j</sup>, A. Meschanin<sup>ag</sup>, R. Millner<sup>w</sup>, N.G. Minaev<sup>ag</sup>, S. Mioduszewski<sup>ap</sup>, A. Mischke<sup>ab</sup>, J. Mitchell<sup>ak</sup>, B. Mohanty<sup>v,au,\*</sup>, D.A. Morozov<sup>ag</sup>, M.G. Munhoz<sup>al</sup>, B.K. Nandi<sup>o</sup>, C. Nattrass<sup>az</sup>, T.K. Nayak<sup>au</sup>, J.M. Nelson<sup>b</sup>, C. Nepali<sup>s</sup>, P.K. Netrakanti<sup>ah</sup>, M.J. Ng<sup>d</sup>, L.V. Nogach<sup>ag</sup>, S.B. Nurushev<sup>ag</sup>, G. Odyniec<sup>v</sup>, A. Ogawa<sup>c</sup>, H. Okada<sup>c</sup>, V. Okorokov<sup>z</sup>, D. Olson<sup>v</sup>, M. Pachr<sup>k</sup>, B.S. Page<sup>p</sup>, S.K. Pal<sup>au</sup>, Y. Pandit<sup>s</sup>, Y. Panebratsev<sup>l</sup>, T. Pawlak<sup>av</sup>, T. Peitzmann<sup>ab</sup>, V. Perevoztchikov<sup>c</sup>, C. Perkins<sup>d</sup>, W. Peryt<sup>av</sup>, S.C. Phatak<sup>n</sup>, M. Planinic<sup>ba</sup>, J. Pluta<sup>av</sup>, N. Poljak<sup>ba</sup>, A.M. Poskanzer<sup>v</sup>, B.V.K.S. Potukuchi<sup>r</sup>, D. Prindle<sup>aw</sup>, C. Pruneau<sup>ax</sup>, N.K. Pruthi<sup>ae</sup>, J. Putschke<sup>az</sup>, R. Raniwala<sup>aj</sup>, S. Raniwala<sup>aj</sup>, R.L. Ray<sup>aq</sup>, R. Redwine<sup>w</sup>, R. Reed<sup>e</sup>, A. Ridiger<sup>z</sup>, H.G. Ritter<sup>v</sup>, J.B. Roberts<sup>ak</sup>, O.V. Rogachevskiy<sup>l</sup>, J.L. Romero<sup>e</sup>, A. Rose<sup>v</sup>, C. Roy<sup>ao</sup>, L. Ruan<sup>c</sup>, M.J. Russcher<sup>ab</sup>, V. Rykov<sup>s</sup>, R. Sahoo<sup>ao</sup>, I. Sakrejda<sup>v</sup>, T. Sakuma<sup>w</sup>, S. Salur<sup>v</sup>, J. Sandweiss<sup>az</sup>, M. Sarsour<sup>ap</sup>, I. Savin<sup>m</sup>, J. Schambach<sup>aq</sup>, R.P. Scharenberg<sup>ah</sup>, N. Schmitz<sup>x</sup>, J. Seger<sup>j</sup>, I. Selyuzhenkov<sup>p</sup>, P. Seyboth<sup>x</sup>, A. Shabetai<sup>q</sup>, E. Shahaliev<sup>l</sup>, M. Shao<sup>am</sup>, M. Sharma<sup>ax</sup>, S.S. Shi<sup>ay</sup>, X.-H. Shi<sup>an</sup>, E. Sichtermann<sup>v</sup>, F. Simon<sup>x</sup>, R.N. Singaraju<sup>au</sup>, M.J. Skoby<sup>ah</sup>, N. Smirnov<sup>az</sup>, R. Snellings<sup>ab</sup>, P. Sorensen<sup>c</sup>, J. Sowinski<sup>p</sup>, H.M. Spinka<sup>a</sup>, B. Srivastava<sup>ah</sup>, A. Stadnik<sup>l</sup>, T.D.S. Stanislaus<sup>at</sup>, D. Staszak<sup>f</sup>, M. Strikhanov<sup>z</sup>, B. Stringfellow<sup>ah</sup>, A.A.P. Suaide<sup>al</sup>, M.C. Suarez<sup>i</sup>, N.L. Subba<sup>s</sup>, M. Sumbera<sup>k</sup>, X.M. Sun<sup>v</sup>, Y. Sun<sup>am</sup>, Z. Sun<sup>u</sup>, B. Surrow<sup>w</sup>, T.J.M. Symons<sup>v</sup>, A. Szanto de Toledo<sup>al</sup>, J. Takahashi<sup>g</sup>, A.H. Tang<sup>c</sup>, Z. Tang<sup>am</sup>, T. Tarnowsky<sup>ah</sup>, D. Thein<sup>aq</sup>, J.H. Thomas<sup>v</sup>, J. Tian<sup>an</sup>,

A.R. Timmins<sup>ax</sup>, S. Timoshenko<sup>z</sup>, D. Tlusty<sup>k</sup>, M. Tokarev<sup>l</sup>, T.A. Trainor<sup>aw</sup>, V.N. Tram<sup>v</sup>, A.L. Trattner<sup>d</sup>, S. Trentalange<sup>f</sup>, R.E. Tribble<sup>ap</sup>, O.D. Tsai<sup>f</sup>, J. Ulery<sup>ah</sup>, T. Ullrich<sup>c</sup>, D.G. Underwood<sup>a</sup>, G. Van Buren<sup>c</sup>, M. van Leeuwen<sup>ab</sup>, A.M. Vander Molen<sup>y</sup>, J.A. Vanfossen Jr.<sup>s</sup>, R. Varma<sup>o</sup>, G.M.S. Vasconcelos<sup>g</sup>, I.M. Vasilevski<sup>m</sup>, A.N. Vasiliev<sup>ag</sup>, F. Videbaek<sup>c</sup>, S.E. Vigdor<sup>p</sup>, Y.P. Viyogi<sup>n</sup>, S. Vokal<sup>l</sup>, S.A. Voloshin<sup>ax</sup>, M. Wada<sup>ap</sup>, W.T. Waggoner<sup>j</sup>, M. Walker<sup>w</sup>, F. Wang<sup>ah</sup>, G. Wang<sup>f</sup>, J.S. Wang<sup>u</sup>, Q. Wang<sup>ah</sup>, X. Wang<sup>ar</sup>, X.L. Wang<sup>am</sup>, Y. Wang<sup>ar</sup>, J.C. Webb<sup>at</sup>, G.D. Westfall<sup>y</sup>, C. Whitten Jr.<sup>f</sup>, H. Wieman<sup>v</sup>, S.W. Wissink<sup>p</sup>, R. Witt<sup>as</sup>, Y. Wu<sup>ay</sup>, N. Xu<sup>v</sup>, Q.H. Xu<sup>v</sup>, Y. Xu<sup>am</sup>, Z. Xu<sup>c</sup>, P. Yepes<sup>ak</sup>, I.-K. Yoo<sup>ai</sup>, Q. Yue<sup>ar</sup>, M. Zawisza<sup>av</sup>, H. Zbroszczyk<sup>av</sup>, W. Zhan<sup>u</sup>, H. Zhang<sup>c</sup>, S. Zhang<sup>an</sup>, W.M. Zhang<sup>s</sup>, Y. Zhang<sup>am</sup>, Z.P. Zhang<sup>am</sup>, Y. Zhao<sup>am</sup>, C. Zhong<sup>an</sup>, J. Zhou<sup>ak</sup>, R. Zoulkarneev<sup>m</sup>, Y. Zoulkarneeva<sup>m</sup>, J.X. Zuo<sup>an</sup>

<sup>a</sup> Argonne National Laboratory, Argonne, IL 60439, United States

<sup>b</sup> University of Birmingham, Birmingham, United Kingdom

<sup>c</sup> Brookhaven National Laboratory, Upton, NY 11973, United States

<sup>d</sup> University of California, Berkeley, CA 94720, United States

<sup>e</sup> University of California, Davis, CA 95616, United States

<sup>f</sup> University of California, Los Angeles, CA 90095, United States

<sup>g</sup> Universidade Estadual de Campinas, Sao Paulo, Brazil

<sup>h</sup> Carnegie Mellon University, Pittsburgh, PA 15213, United States

<sup>i</sup> University of Illinois at Chicago, Chicago, IL 60607, United States

<sup>j</sup> Creighton University, Omaha, NE 68178, United States

<sup>k</sup> Nuclear Physics Institute AS CR, 250 68 Řež/Prague, Czech Republic

<sup>l</sup> Laboratory for High Energy (JINR), Dubna, Russia

<sup>m</sup> Particle Physics Laboratory (JINR), Dubna, Russia

<sup>n</sup> Institute of Physics, Bhubaneswar 751005, India

<sup>o</sup> Indian Institute of Technology, Mumbai, India

<sup>p</sup> Indiana University, Bloomington, IN 47408, United States

<sup>q</sup> Institut de Recherches Subatomiques, Strasbourg, France

<sup>r</sup> University of Jammu, Jammu 180001, India

<sup>s</sup> Kent State University, Kent, OH 44242, United States

<sup>t</sup> University of Kentucky, Lexington, KY 40506-0055, United States

<sup>u</sup> Institute of Modern Physics, Lanzhou, China

<sup>v</sup> Lawrence Berkeley National Laboratory, Berkeley, CA 94720, United States

<sup>w</sup> Massachusetts Institute of Technology, Cambridge, MA 02139-4307, United States

<sup>x</sup> Max-Planck-Institut für Physik, Munich, Germany

<sup>y</sup> Michigan State University, East Lansing, MI 48824, United States

<sup>z</sup> Moscow Engineering Physics Institute, Moscow, Russia

<sup>aa</sup> City College of New York, New York City, NY 10031, United States

<sup>ab</sup> NIKHEF and Utrecht University, Amsterdam, The Netherlands

<sup>ac</sup> Ohio State University, Columbus, OH 43210, United States

<sup>ad</sup> Old Dominion University, Norfolk, VA 23529, United States

<sup>ae</sup> Panjab University, Chandigarh 160014, India

<sup>af</sup> Pennsylvania State University, University Park, PA 16802, United States

<sup>ag</sup> Institute of High Energy Physics, Protvino, Russia

<sup>ah</sup> Purdue University, West Lafayette, IN 47907, United States

<sup>ai</sup> Pusan National University, Pusan, Republic of Korea

<sup>aj</sup> University of Rajasthan, Jaipur 302004, India

<sup>ak</sup> Rice University, Houston, TX 77251, United States

<sup>al</sup> Universidade de Sao Paulo, Sao Paulo, Brazil

<sup>am</sup> University of Science & Technology of China, Hefei 230026, China

<sup>an</sup> Shanghai Institute of Applied Physics, Shanghai 201800, China

<sup>ao</sup> SUBATECH, Nantes, France

<sup>ap</sup> Texas A&M University, College Station, TX 77843, United States

<sup>aq</sup> University of Texas, Austin, TX 78712, United States

<sup>ar</sup> Tsinghua University, Beijing 100084, China

<sup>as</sup> United States Naval Academy, Annapolis, MD 21402, United States

<sup>at</sup> Valparaiso University, Valparaiso, IN 46383, United States

<sup>au</sup> Variable Energy Cyclotron Centre, Kolkata 700064, India

<sup>av</sup> Warsaw University of Technology, Warsaw, Poland

<sup>aw</sup> University of Washington, Seattle, WA 98195, United States

<sup>ax</sup> Wayne State University, Detroit, MI 48201, United States

<sup>ay</sup> Institute of Particle Physics, CCNU (HZNU), Wuhan 430079, China

<sup>az</sup> Yale University, New Haven, CT 06520, United States

<sup>ba</sup> University of Zagreb, Zagreb, HR-10002, Croatia

## ARTICLE INFO

### Article history:

Received 28 October 2008

Received in revised form 18 February 2009

Accepted 22 February 2009

Available online 25 February 2009

Editor: V. Metag

### Keywords:

Particle production

Strangeness enhancement

Canonical suppression

## ABSTRACT

We study the beam-energy and system-size dependence of  $\phi$  meson production (using the hadronic decay mode  $\phi \rightarrow K^+ K^-$ ) by comparing the new results from Cu + Cu collisions and previously reported Au + Au collisions at  $\sqrt{s_{NN}} = 62.4$  and 200 GeV measured in the STAR experiment at RHIC. Data presented in this Letter are from mid-rapidity ( $|y| < 0.5$ ) for  $0.4 < p_T < 5$  GeV/c. At a given beam energy, the transverse momentum distributions for  $\phi$  mesons are observed to be similar in yield and shape for Cu + Cu and Au + Au colliding systems with similar average numbers of participating nucleons. The  $\phi$  meson yields in nucleus–nucleus collisions, normalized by the average number of participating nucleons, are found to be enhanced relative to those from  $p + p$  collisions. The enhancement for  $\phi$  mesons lies between strange hadrons having net strangeness = 1 ( $K^-$  and  $\bar{\Lambda}$ ) and net strangeness = 2 ( $\Xi$ ). The enhancement for  $\phi$  mesons is observed to be higher at  $\sqrt{s_{NN}} = 200$  GeV compared to 62.4 GeV. These

observations for the produced  $\phi(s\bar{s})$  mesons clearly suggest that, at these collision energies, the source of enhancement of strange hadrons is related to the formation of a dense partonic medium in high energy nucleus–nucleus collisions and cannot be alone due to canonical suppression of their production in smaller systems.

© 2009 Elsevier B.V. Open access under CC BY license.

## 1. Introduction

Experimental results from the Relativistic Heavy Ion Collider (RHIC) have confirmed the formation of a hot and dense medium in the initial stages of high-energy heavy-ion collisions [1]. Thus one of the prerequisites for the formation of a Quark–Gluon Plasma (QGP) [2] in such collisions has been established. High statistics data on  $\phi$  meson elliptic flow and yields as a function of transverse momentum ( $p_T$ ) have been used to support the picture of formation of a hot and dense medium with partonic collectivity at RHIC [3,4]. Evidence of  $\phi$  mesons being formed by the coalescence of seemingly thermalized  $s\bar{s}$ -quarks in central Au + Au collisions has also been presented [3].

Several interesting features were also observed in the centrality dependence of  $\phi$  meson production in Au + Au collisions at 200 GeV. As one goes from central collisions (average number of participants,  $\langle N_{\text{part}} \rangle > 166$ ) to peripheral collisions ( $\langle N_{\text{part}} \rangle < 77$ ), the  $p_T$  spectra showed a gradual evolution from an exponential shape to a shape which requires an additional power law type of behavior at higher  $p_T$  ( $> 3$  GeV/c) [3,5]. At the same time, the average transverse momentum ( $\langle p_T \rangle$ ) of  $\phi$  mesons, dominated by the transverse momentum distribution at low  $p_T$ , showed no significant collision centrality dependence in Au + Au collisions, unlike what has been seen for other particles of similar mass such as anti-protons ( $\bar{p}$ ) [5,6]. The  $N(\phi)/N(K^-)$  ratio was observed to be independent of collision centrality in Au + Au collisions, in contrast to predictions from microscopic transport models like RQMD and UrQMD [7]. Both of these results led to the conclusion that  $\phi$  meson production may not be from  $K\bar{K}$  coalescence and  $\phi$  mesons may have decoupled early on in the collisions [5,8].

The linear increase of the  $N(\Omega)/N(\phi)$  ratio with  $p_T$  was proposed as an observable to test the recombination picture and hence also provided a test for thermalization in heavy-ion collisions [9]. A distinct trend was observed in the centrality dependence of this ratio vs.  $p_T$  in Au + Au collisions [3]. With decreasing centrality, the observed  $N(\Omega)/N(\phi)$  ratio seems to turn over at successively lower values of  $p_T$  indicating a smaller contribution from thermal quark coalescence in more peripheral collisions. Furthermore, in lower energy collisions at the SPS [10] and AGS [11], it was observed that the relative strangeness production increases with  $N_{\text{part}}$ . For similar  $N_{\text{part}}$ , the increase was found to be slower for larger colliding ions. The possible reason was related to variations of space–time density of the participating nucleons and the increase in collision density (interactions per  $\text{fm}^3$ ) towards the center of the reaction volume [10,11]. The measurement of  $\phi$  production in Cu + Cu collisions, in which systems with  $N_{\text{part}} < 128$  are created, is therefore expected to provide more precise data to further probe these centrality and colliding ion size dependent features.

In this Letter we report the first results of  $\phi$  meson production for rapidities  $|y| < 0.5$  and  $0.4 < p_T < 5$  GeV/c in Cu + Cu collisions at  $\sqrt{s_{\text{NN}}} = 62.4$  and 200 GeV. The data were taken by the STAR experiment at RHIC [12]. A detailed comparative study of the

energy and system size dependence of  $\phi$  meson production ( $p_T$  spectra, rapidity density and  $\langle p_T \rangle$ ) is carried out using both the Cu + Cu and Au + Au data.

Several possible mechanisms of  $\phi$  meson production in nucleus–nucleus collisions have been reported in the literature [9,13–15]. Some of these are supported by the experimental data which is not true with others [3]. In a QGP, thermal  $s$  and  $\bar{s}$  quarks can be produced by gluon–gluon interactions [13]. These interactions could occur very rapidly and the  $s$ -quark abundance would equilibrate. During hadronization, the  $s$  and  $\bar{s}$  quarks from the plasma coalesce to form  $\phi$  mesons. Production by this process is not suppressed as per the OZI (Okubo–Zweig–Izuka) rule [16]. This, coupled with large abundances of strange quarks in the plasma, may lead to a dramatic increase in the production of  $\phi$  mesons and other strange hadrons relative to non-QGP  $p + p$  collisions [17]. Alternative ideas of canonical suppression of strangeness in small systems as a source of strangeness enhancement in high energy heavy-ion collisions have been proposed for other strange hadrons (e.g.  $\Lambda$ ,  $\Xi$  and  $\Omega$ ) [18]. The strangeness conservation laws require the production of an  $\bar{s}$ -quark for each  $s$ -quark in the strong interaction. The main argument in such canonical models is that the energy and space–time extensions in smaller systems may not be sufficiently large. This leads to a suppression of strange hadron production in small collision systems. These statistical models fit the data reasonably well [19]. According to these models, strangeness enhancement in nucleus–nucleus collisions, relative to  $p + p$  collisions, should increase with the strange quark content of the hadrons. This enhancement is predicted to decrease with increasing beam energy [20]. So far, discriminating between the two scenarios (strange hadron enhancement being due to dense partonic medium formed in heavy-ion collisions or due to canonical suppression of their production in  $p + p$  collisions) using the available experimental data has been, to some extent, ambiguous. Enhancement of  $\phi(s\bar{s})$  production (zero net strangeness) in Cu + Cu and Au + Au relative to  $p + p$  collisions would clearly indicate the formation of a dense partonic medium in these collisions. This would then rule out canonical suppression effects being the most likely cause for the observed enhancement in other strange hadrons [21] in high energy heavy-ion collisions.

## 2. Experiment and analysis

The data presented here were taken at RHIC in 2004 (Au + Au) and 2005 (Cu + Cu) using the STAR detector [12]. The analysis presented is from the data taken by the Time Projection Chamber (TPC) [22]. The TPC magnetic field was 0.5 Tesla. Data were taken in both field configurations. The trigger conditions and number of events analyzed for different colliding systems at  $\sqrt{s_{\text{NN}}} = 62.4$  GeV and 200 GeV are given in Table 1. The  $\phi$  meson spectra for Au + Au collisions at 200 GeV using these data sets have been presented elsewhere [3]. Centrality selection for the Au + Au and Cu + Cu collisions utilized the uncorrected charged particle multiplicity for pseudorapidities  $|\eta| < 0.5$ , measured by the TPC. Table 2 shows the  $\langle N_{\text{part}} \rangle$  and  $\langle N_{\text{bin}} \rangle$  values calculated using a Glauber model for different centralities for Au + Au and Cu + Cu collisions at 62.4 and 200 GeV. The values for Au + Au collisions at 62.4 GeV were published previously [23].

\* Corresponding author at: Variable Energy Cyclotron Centre, Kolkata 700064, India.

E-mail address: bedanga@rcf.rhic.bnl.gov (B. Mohanty).

The  $\phi$  meson yield in each  $p_T$  bin was extracted from the invariant mass ( $M_{\text{inv}}$ ) distributions of  $K^+K^-$  candidates after the subtraction of the combinatorial background estimated using the event mixing technique [3,5,24]. The charged kaons were identified through their ionization energy loss in the TPC. The typical signal/background ratio in Cu + Cu collisions varies from  $\sim 0.03$  for  $p_T = 0.45$  GeV/c to around 0.009 for  $p_T = 2.8$  GeV/c for 0–10% collision centrality. This ratio varies between 0.11 to 0.06 for  $p_T$  between 0.45 to 2.8 GeV/c for 50–60% collision centrality. Fig. 1 shows a typical, background subtracted,  $K^+K^-$   $M_{\text{inv}}$  distribution as obtained for 200 GeV Cu + Cu collisions. The resultant distribution is well described by a Breit-Wigner function (solid line) plus a linear background function (dashed line). The form of the Breit-Wigner function is  $\frac{dN}{dM_{\text{inv}}} = \frac{C\Gamma}{(M_{\text{inv}} - m_\phi)^2 + \Gamma^2/4}$ , where  $C$  is the area under the mass peak,  $\Gamma$  is the full width at half maximum for the distribution in GeV/ $c^2$  and  $m_\phi$  is the mass of the  $\phi$  meson. Fig. 1 also shows that for  $p_T > 0.7$  GeV/c, the mass peak position of the  $\phi$  meson agrees well with the PDG value of 1.0194 GeV [25]. For  $p_T < 1.2$  GeV/c there is a monotonic drop in the value of the fitted mass value with decreasing  $p_T$ , reaching (mass  $\phi$  fitted – mass  $\phi$  PDG) =  $-2.5$  MeV at  $p_T = 0.5$  GeV/c. The reconstructed invariant mass distribution of the  $\phi$  meson is wider than the PDG value (4.26 MeV/ $c^2$ ), decreasing from 9 MeV/ $c^2$  to 4.26 MeV/ $c^2$  with increasing  $p_T$  [26]. The variations in the position of the  $\phi$  invariant mass peak and its width, at low  $p_T$ , are consistent with the simulation values and are understood within the scope of the detector resolution effects [24]. To understand these effects,  $\phi$  decays to  $K^+K^-$  and detector response were studied within the STAR GEANT framework [27]. The resulting simulated signals were then embedded into real events before being processed by the standard STAR event reconstruction. These data were then processed like real data and analyzed to reconstruct the embedded  $\phi$  [3,5,24,26]. Embedding simulations were also used to obtain the  $\phi$  meson acceptance and reconstruction efficiency [24,26]. The product of the acceptance and reconstruction efficiency was found to increase from 3% at  $p_T = 0.5$  GeV/c to about 40% at  $p_T = 3$  GeV/c for central Cu + Cu collisions. The centrality dependence of these values were found to be small for Cu + Cu collisions. At higher  $p_T$  (3–5 GeV/c), the efficiency was found to remain constant. The other important corrections applied

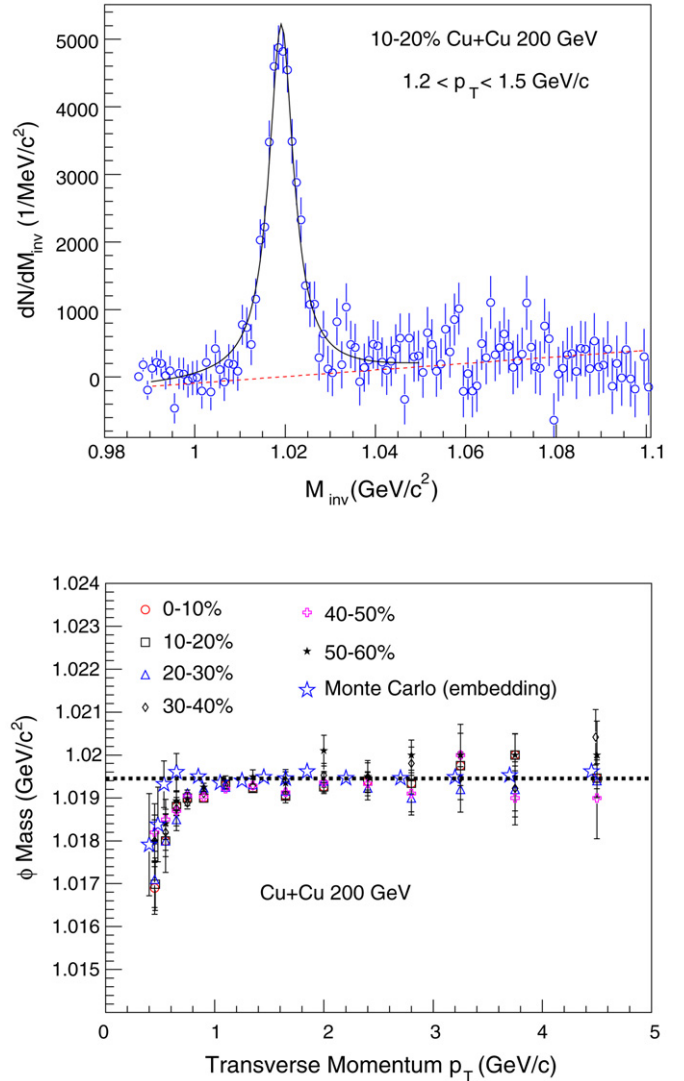


**Fig. 1.** Upper panel: A typical  $\phi$  meson mass peak in Cu + Cu collisions at 200 GeV obtained from the  $K^+K^-$  invariant mass distribution after subtracting the combinatorial background using mixed events. The distribution is fitted to a Breit-Wigner function (solid line) and a linear background function (dashed line) to extract the yields. The errors shown are statistical. Lower panel:  $\phi$  meson mass peak position as a function of  $p_T$  for various collision centralities in Cu + Cu collisions at 200 GeV. Also shown are the results from Monte Carlo calculations for 0–60% centrality using embedding techniques (see text for more details) shifted by 50 MeV/c in  $p_T$  for clarity of presentation. The dashed line corresponds to the PDG value of 1.0194 GeV/ $c^2$  [25].

**Table 1**

Collision systems, beam energies, number of events and trigger conditions.

Collision system	$\sqrt{s_{\text{NN}}}$ (GeV)	Number of events	Trigger condition
Cu + Cu	62.4	$8.8 \times 10^6$	Minimum bias (0–60%)
Cu + Cu	200	$1.5 \times 10^7$	Minimum bias (0–60%)
Au + Au	62.4	$6.2 \times 10^6$	Minimum bias (0–80%)
Au + Au	200	$1.35 \times 10^7$	Minimum bias (0–80%)
Au + Au	200	$1.0 \times 10^7$	Central trigger (0–12%)

**Table 2**

The average numbers of participating nucleons ( $\langle N_{\text{part}} \rangle$ ) and binary collisions ( $\langle N_{\text{bin}} \rangle$ ) for various collision centralities in Au + Au and Cu + Cu collisions at  $\sqrt{s_{\text{NN}}} = 62.4$  and 200 GeV.

% cs	$\langle N_{\text{part}}^{\text{AuAu}} \rangle$	$\langle N_{\text{bin}}^{\text{AuAu}} \rangle$	$\langle N_{\text{part}}^{\text{AuAu}} \rangle$	$\langle N_{\text{bin}}^{\text{AuAu}} \rangle$	$\langle N_{\text{part}}^{\text{CuCu}} \rangle$	$\langle N_{\text{bin}}^{\text{CuCu}} \rangle$	$\langle N_{\text{part}}^{\text{CuCu}} \rangle$	$\langle N_{\text{bin}}^{\text{CuCu}} \rangle$
	200 GeV	200 GeV	62.4 GeV	62.4 GeV	200 GeV	200 GeV	62.4 GeV	62.4 GeV
0–10	$325.9^{+5.5}_{-4.3}$	$939.4^{+72.1}_{-63.7}$	$320.3^{+5.7}_{-4.5}$	$809.4^{+64.9}_{-59.0}$	$99.0^{+1.5}_{-1.2}$	$188.8^{+15.4}_{-13.4}$	$96.4^{+1.1}_{-2.6}$	$161.8^{+12.1}_{-7.5}$
10–20	$234.5^{+9.0}_{-7.8}$	$590.9^{+60.8}_{-53.7}$	$229.0^{+9.2}_{-7.7}$	$511.8^{+54.9}_{-48.2}$	$74.6^{+1.3}_{-1.0}$	$123.6^{+9.4}_{-8.3}$	$72.2^{+0.6}_{-1.9}$	$107.5^{+6.3}_{-8.6}$
20–30	$166.6^{+10.1}_{-9.6}$	$368.5^{+47.0}_{-44.9}$	$162.0^{+10.0}_{-9.5}$	$320.9^{+43.0}_{-39.2}$	$53.7^{+1.0}_{-0.7}$	$77.6^{+5.4}_{-4.7}$	$51.8^{+0.5}_{-1.2}$	$68.4^{+3.6}_{-4.7}$
30–40	$115.5^{+9.6}_{-9.6}$	$220.1^{+35.1}_{-34.8}$	$112.0^{+9.6}_{-9.1}$	$193.5^{+31.4}_{-30.4}$	$37.8^{+0.7}_{-0.5}$	$47.7^{+2.8}_{-2.7}$	$36.2^{+0.4}_{-0.8}$	$42.3^{+2.0}_{-2.6}$
40–50	$76.7^{+9.0}_{-9.1}$	$123.5^{+24.0}_{-25.4}$	$74.2^{+9.0}_{-8.5}$	$109.3^{+22.1}_{-21.8}$	$26.2^{+0.5}_{-0.4}$	$29.2^{+1.6}_{-1.4}$	$24.9^{+0.4}_{-0.6}$	$25.9^{+1.0}_{-1.5}$
50–60	$47.3^{+7.6}_{-8.1}$	$63.9^{+15.5}_{-16.8}$	$45.8^{+7.0}_{-7.1}$	$56.6^{+15.0}_{-14.3}$	$17.2^{+0.4}_{-0.2}$	$16.8^{+0.9}_{-0.7}$	$16.3^{+0.4}_{-0.3}$	$15.1^{+0.6}_{-0.6}$
60–70	$26.9^{+5.5}_{-6.5}$	$29.5^{+9.5}_{-9.8}$	$25.9^{+5.6}_{-5.6}$	$26.8^{+8.8}_{-9.0}$	–	–	–	–
70–80	$14.1^{+3.6}_{-4.0}$	$12.3^{+4.7}_{-4.8}$	$13.0^{+3.4}_{-4.6}$	$11.2^{+3.7}_{-4.8}$	–	–	–	–



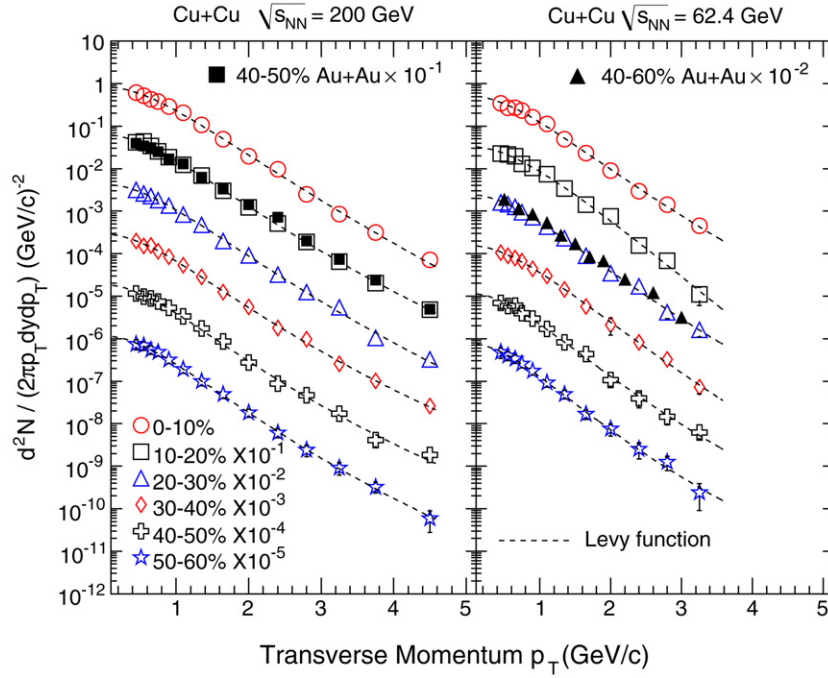


**Fig. 2.** Midrapidity ( $|y| < 0.5$ ) transverse momentum spectra of  $\phi$  mesons for various collision centrality classes for Cu + Cu collisions at  $\sqrt{s_{NN}} = 62.4$  and 200 GeV. To study the system size dependence, comparison of 40–50% Au + Au spectra to 10–20% Cu + Cu spectra at 200 GeV, and 40–60% Au + Au spectra to 20–30% Cu + Cu spectra at 62.4 GeV are shown. These centralities for the two colliding systems have similar  $\langle N_{part} \rangle$  values as outlined in Table 2. The errors represent the statistical and systematic errors added in quadrature. They are found to be within the symbol size. The spectra are fitted to a Lévy function discussed in the text.

to the data were related to the vertex finding efficiency which was  $\sim 92.5\%$  and the correction for branching ratio of 49.2% for the channel  $\phi \rightarrow K^+K^-$ . A more detailed description of the  $\phi$  meson mass peak position, width of the  $\phi$  meson invariant mass distribution, variation of the reconstruction efficiency with collision centrality and  $p_T$ , and the general procedure for obtaining the signal and constructing mixed events are discussed elsewhere [26].

The systematic errors for the  $\phi$  meson spectral measurements in Cu + Cu collisions include uncertainties from the following sources: Uncertainties in  $\phi$  meson reconstruction efficiency ( $\sim 8\text{--}14\%$ ), kaon identification from  $dE/dx$  (8%), kaon energy loss corrections ( $\sim 3\text{--}4\%$ ), residual background shape (4%) and magnetic field configuration ( $\sim 3\%$ ). The systematic errors from all the above sources have been added in quadrature. Systematic errors for the  $\phi$  meson spectra are similar at both energies (62.4 and 200 GeV). The total systematic errors for  $\phi$  yields at both energies are estimated to be  $\lesssim 18\%$  over the entire  $p_T$  range studied. A discussion on systematic errors for Au + Au collisions,  $dN/dy$ , and  $\langle p_T \rangle$  can be found in Refs. [3,5,26].

### 3. Transverse momentum distributions and yields

Fig. 2 shows the  $\phi$  meson yields from Cu + Cu collisions at 62.4 and 200 GeV for  $0.4 < p_T < 5$  GeV/c and various collision centralities. The spectra are well described by a Lévy function of the form  $\frac{d^2N}{2\pi p_T dp_T dy} = \frac{A}{[1 + (m_T - m_\phi)/n T_{Levy}]^n}$ , where  $m_T = \sqrt{p_T^2 + m_\phi^2}$ .  $A$ ,  $T_{Levy}$ , and  $n$  are the parameters of the function. In the limiting case of  $1/n \rightarrow 0$ , the Lévy distribution approaches an exponential function. The parameters  $T_{Levy}$  and  $n$  have similar values for the Cu + Cu and Au + Au systems with similar  $\langle N_{part} \rangle$  at 200 GeV. This reflects the similar shape for the  $\phi$  meson spectra in both collision systems at a given energy and  $\langle N_{part} \rangle$ . A comparison of  $\phi$  mesons spectra for 40–50% central Au + Au ( $\langle N_{part} \rangle = 76.7$ ) and 10–20% central Cu + Cu ( $\langle N_{part} \rangle = 74.6$ ) collisions at 200 GeV is shown in Fig. 2 (left panel). Similar results for 40–60% central Au + Au ( $\langle N_{part} \rangle = 59.9$ ) and 20–30% central Cu + Cu ( $\langle N_{part} \rangle = 51.8$ ) col-

lisions at 62.4 GeV are also shown in the same figure on the right panel. The ratios of the  $\phi$  meson  $p_T$  spectra for Au + Au and Cu + Cu systems with similar  $\langle N_{part} \rangle$  agree with one within  $\sim 10\%$ . This is further quantified by studying their rapidity density ( $dN/dy$ ) and  $\langle p_T \rangle$  for both colliding systems.

Fig. 3 shows  $dN/dy$ ,  $dN/dy/\langle N_{part} \rangle$  and  $\langle p_T \rangle$  as a function of  $\langle N_{part} \rangle$  for Cu + Cu and Au + Au collisions at 62.4 and 200 GeV. The Lévy distribution is used to get the estimate of yields for the unmeasured  $p_T$  ranges of  $p_T < 0.4$  GeV/c and  $p_T > 4.5$  GeV/c ( $p_T > 3.5$  GeV/c for Cu + Cu collisions at 62.4 GeV) at midrapidity. Results from  $p + p$  at 200 GeV and 63 GeV, obtained from the STAR [5] and ISR [29] experiments respectively, are also included for comparison. At 63 GeV the  $d\sigma/dy$  for  $\phi$  mesons at  $0 < y < 0.33$  was reported to be  $0.44 \pm 0.11(\text{sys}) \pm 0.1(\text{stat})$  mb. These data, together with values of 36 and 42 mb for  $p + p$  inelastic cross-sections at 63 and 200 GeV respectively, have been used to get the corresponding  $dN/dy$  values shown in the figure. The  $dN/dy$  and  $\langle p_T \rangle$  values as obtained for the Cu + Cu collisions are also presented in Table 3. Both at 62.4 and 200 GeV, all three quantities  $dN/dy$ ,  $dN/dy/\langle N_{part} \rangle$  and  $\langle p_T \rangle$  scale with  $\langle N_{part} \rangle$ . These findings seem to indicate that the general features of  $\phi$  meson production characterized in terms of  $dN/dy$  and  $\langle p_T \rangle$  at a given energy (62.4 or 200 GeV) do not depend on the colliding ion species studied, but depend on the  $\langle N_{part} \rangle$  of the collision. It will be interesting to see whether the same is true for other produced hadrons at RHIC. However, for a given  $\langle N_{part} \rangle$ , both  $dN/dy$  and  $\langle p_T \rangle$  are observed to be lower for 62.4 GeV when compared to 200 GeV. This is in contrast to what has been seen at lower energies at AGS and SPS with smaller colliding systems [10,11]. At those lower energies, for similar  $\langle N_{part} \rangle$ , the strange hadron production was higher for smaller colliding systems compared to larger colliding systems. While at RHIC, due to higher center of mass energy, a hotter and denser medium is expected to form with a very low net baryon density at midrapidity [1], leading to the observed differences. Recent theoretical calculations based on decomposing the total volume in heavy-ion collisions to consist of a core (high den-

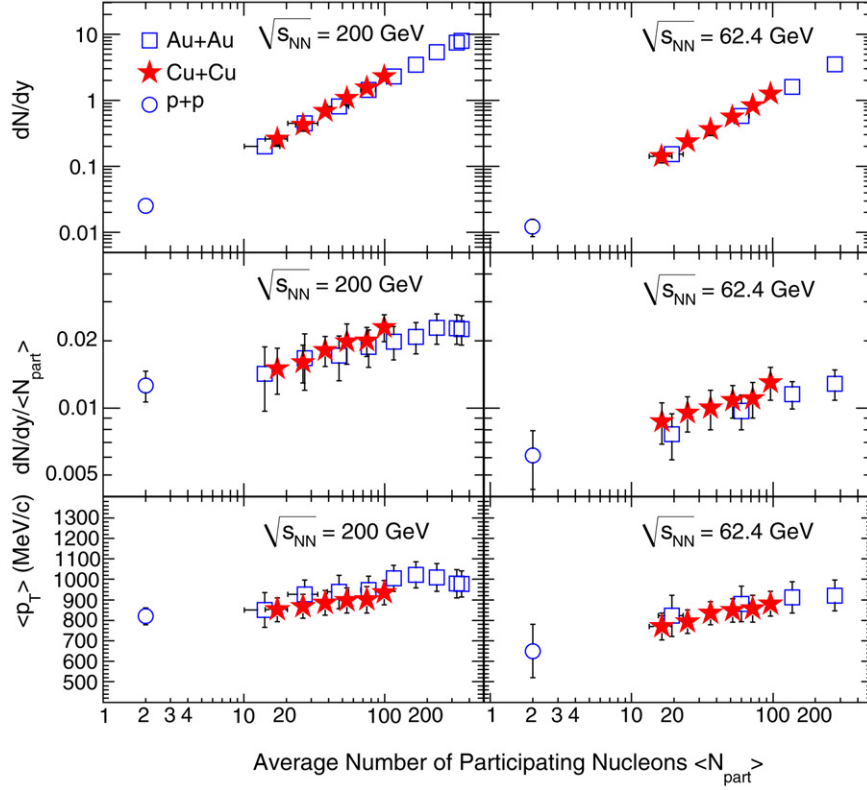


**Fig. 3.** Upper panels:  $dN/dy$  at midrapidity for  $\phi$  mesons for various collision centrality classes in Cu + Cu and Au + Au at  $\sqrt{s_{NN}} = 200$  GeV and 62.4 GeV. Also shown are the results from  $p + p$  collisions. Middle panels: Same as above, but for  $dN/dy/\langle N_{part} \rangle$ . Lower panels: Average transverse momentum ( $\langle p_T \rangle$ ) for  $\phi$  mesons at midrapidity for various event centrality classes for Cu + Cu and Au + Au collisions at  $\sqrt{s_{NN}} = 62.4$  GeV and 200 GeV. The  $\langle p_T \rangle$  for  $\phi$  mesons in  $p + p$  collisions are also shown. The error bars represent the statistical and systematic errors added in quadrature.

**Table 3**  
 $dN/dy$  and  $\langle p_T \rangle$  for  $\phi$  mesons produced in Cu + Cu collisions at  $\sqrt{s_{NN}} = 200$  and 62.4 GeV for various collision centralities. The errors mentioned are statistical (first error) and systematic (second error).

% centrality	$dN/dy$ 200 GeV	$dN/dy$ 62.4 GeV	$\langle p_T \rangle$ (MeV/c) 200 GeV	$\langle p_T \rangle$ (MeV/c) 62.4 GeV
0–10	$2.3 \pm 0.03 \pm 0.3$	$1.3 \pm 0.03 \pm 0.2$	$935 \pm 8 \pm 59$	$881 \pm 10 \pm 60$
10–20	$1.6 \pm 0.02 \pm 0.2$	$0.8 \pm 0.02 \pm 0.1$	$901 \pm 9 \pm 63$	$857 \pm 9 \pm 64$
20–30	$1.1 \pm 0.02 \pm 0.2$	$0.6 \pm 0.01 \pm 0.1$	$897 \pm 9 \pm 61$	$848 \pm 12 \pm 56$
30–40	$0.7 \pm 0.01 \pm 0.1$	$0.4 \pm 0.009 \pm 0.1$	$885 \pm 9 \pm 59$	$835 \pm 15 \pm 55$
40–50	$0.4 \pm 0.007 \pm 0.1$	$0.24 \pm 0.005 \pm 0.04$	$869 \pm 9 \pm 58$	$793 \pm 13 \pm 55$
50–60	$0.26 \pm 0.009 \pm 0.05$	$0.14 \pm 0.004 \pm 0.03$	$852 \pm 11 \pm 57$	$771 \pm 14 \pm 54$

sity part) and corona (low density part) are able to explain similar yields of  $\phi$ -mesons in Au + Au and Cu + Cu collisions at similar  $\langle N_{part} \rangle$  at RHIC [28].

#### 4. Nuclear modification factor

Now we look at the  $p_T$  dependences of the nuclear modification factor for the  $\phi$  meson, both in terms of  $N_{part}$  and  $N_{bin}$ . For  $N_{part}$ , this factor is given by

$$R_{AA}^{N_{part}}(p_T) = \frac{d^2 N_{AA}/dy dp_T / \langle N_{part} \rangle}{d^2 \sigma_{pp}/dy dp_T / \sigma_{pp}^{inel}}.$$

To get the corresponding  $R_{AA}^{N_{bin}}(p_T)$ , one needs to replace  $\langle N_{part} \rangle$  by  $\langle N_{bin} \rangle$  in the above expression. The results, as shown in Figs. 2 and 3 would lead to very similar results on  $R_{AA}^{N_{part}}$  for both Cu + Cu and Au + Au systems for collisions having similar  $\langle N_{part} \rangle$ . In view of this, we only present here a comparison of the nuclear modification factors (in terms of  $N_{bin}$  and  $N_{part}$ ) of  $R_{AA}^{N_{part}}$  and  $R_{AA}^{N_{bin}}$  for Cu + Cu and Au + Au collisions. For such a comparison, only centralities corresponding to similar fraction of total hadronic cross-

section were considered. The  $R_{AA}$  for  $\phi$  mesons in 200 GeV Cu + Cu and Au + Au collisions for 0–10% and 20–30% collision centralities (up to  $p_T = 4$  GeV/c) at 200 GeV are shown in Fig. 4.

Within the errors, the  $R_{AA}^{N_{part}}$  values for 0–10% central Cu + Cu and Au + Au collisions at 200 GeV are seen to be similar in shape and yields. However, for 20–30% collisions and at other collision centralities (which are not shown in the figure) the Au + Au results are higher than Cu + Cu results for most of the  $p_T$  range studied. The results for the central most Cu + Cu and Au + Au collisions studied are consistent with the observation that  $dN/dy/\langle N_{part} \rangle$  and  $\langle p_T \rangle$  are constant as a function of  $\langle N_{part} \rangle$  for  $\langle N_{part} \rangle > 90$  (Fig. 3).

At the same collision centralities, the ratio  $\langle N_{bin}^{AuAu} \rangle / \langle N_{bin}^{CuCu} \rangle$  is about  $\sim 1.5$  times larger than the ratio  $\langle N_{part}^{AuAu} \rangle / \langle N_{part}^{CuCu} \rangle$ . This is reflected in the  $R_{AA}^{N_{bin}}$ . As one can see from Fig. 4,  $R_{AA}^{N_{bin}}$  for 0–10% Cu + Cu is higher than that of Au + Au collisions, for  $p_T < 3.5$  GeV/c. Both the modification factors at  $p_T > 3.5$  GeV/c are below unity, showing the characteristics of parton energy loss in hot and dense medium formed in central heavy-ion collisions. For 20–30% central collisions, the similarity between  $R_{AA}^{N_{bin}}$  for Cu + Cu and Au + Au collisions seems to extend to lower  $p_T$  ( $\sim 1.5$  GeV/c). It may be

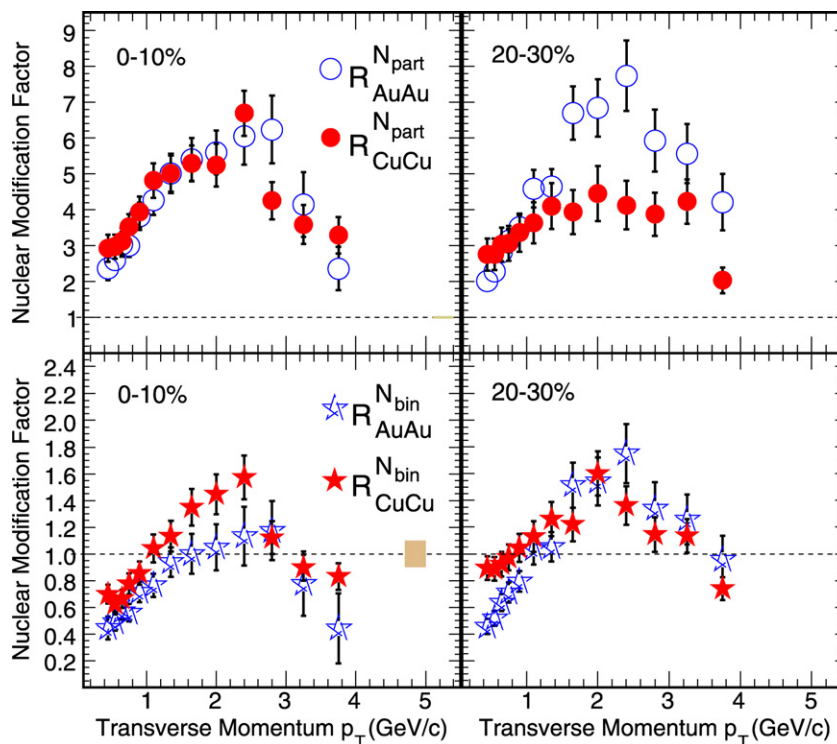


**Fig. 4.** Upper panels:  $N_{\text{part}}$  scaled ( $R_{\text{AA}}^{N_{\text{part}}}$ ) nuclear modification factors as a function of  $p_T$  of  $\phi$  mesons for 0–10% and 20–30% Cu + Cu and Au + Au collisions at  $\sqrt{s_{\text{NN}}} = 200$  GeV. Lower panel: Same as above for  $N_{\text{bin}}$  scaled ( $R_{\text{AA}}^{N_{\text{bin}}}$ ) nuclear modification factor. The error bars represent the statistical and systematic errors added in quadrature. The shaded band in upper panel around 1 at  $p_T = 4.5$ – $5.5$  GeV/c in the right side reflects the uncertainty in  $\langle N_{\text{part}} \rangle$  and that on the lower panel for  $\langle N_{\text{bin}} \rangle$  calculation for central Au + Au collisions. The respective uncertainties for central Cu + Cu collisions are of similar order.

interesting to use the nuclear modification factor of  $\phi$  mesons to investigate the differences in energy loss of quarks and gluons in the medium formed in heavy-ion collisions [30]. This is because  $\phi$  mesons in central collisions are formed from coalescence of  $s$  and  $\bar{s}$  quarks [3], which presumably are formed by gluon interactions in the initial stages of the collision.

### 5. $\phi$ meson production and strangeness enhancement

The ratio of strange hadron production normalized to  $\langle N_{\text{part}} \rangle$  in nucleus–nucleus collisions relative to corresponding results from  $p + p$  collisions at 200 GeV are shown in the upper panel of Fig. 5. The results are plotted as a function of  $\langle N_{\text{part}} \rangle$ .  $K^-$  [31],  $\bar{\Lambda}$  and  $\Xi + \bar{\Xi}$  [21] are found to exhibit an enhancement (value  $> 1$ ) that increases with the number of strange valence quarks. Furthermore, the observed enhancement in these open-strange hadrons increases with collision centrality, reaching a maximum for the most central collisions. However, the enhancement of  $\phi$  meson production from Cu + Cu and Au + Au collisions shows a deviation in ordering in terms of the number of strange constituent quarks. More explicitly, this enhancement is larger than for  $K^-$  and  $\bar{\Lambda}$ , at the same time being smaller than in case of  $\Xi + \bar{\Xi}$ . Despite being different particle types (meson–baryon) and having different masses, the results for  $K^-$  and  $\bar{\Lambda}$  are very similar in the entire centrality region studied. This rules out a baryon–meson effect as being the reason for the deviation of  $\phi$  mesons from the number of strange quark ordering seen in Fig. 5 (upper panel). The observed deviation is also not a mass effect as the enhancement in  $\phi$  meson production is larger than that in  $\bar{\Lambda}$  (which has mass close to that of the  $\phi$ ).

In heavy-ion collisions, the production of  $\phi$  mesons is not canonically suppressed due to its  $s\bar{s}$  structure. In low energy  $p + \bar{p}$  collisions at  $\sqrt{s} = 3.6$  GeV,  $\phi$  meson production is suppressed due to the OZI rule [32]. In  $p + p$  collisions at  $\sqrt{s} = 6.84$  GeV

violation of this rule has been reported [33,34]. At this higher energy,  $\phi$  production through channels accompanied by non-strange hadrons was found to dominate strongly over its production in channels accompanied with strange hadrons. Measurements of  $\phi$  production in proton–nucleus collisions at  $\sqrt{s_{\text{NN}}} = 27.4$  GeV have also shown that it takes place primarily by other than OZI allowed processes [35]. Experiments studying inclusive  $\phi$  production off protons by hadrons at incident momenta 63 and 93 GeV/c have shown similar conclusions [36]. Experiments on the production of  $\phi$  mesons in  $p + p$  collisions near threshold have shown a large enhancement of the cross-section ratio  $\sigma(pp \rightarrow p\phi)/\sigma(pp \rightarrow p\omega)$  [37] compared to that predicted by the OZI rule [38]. This ratio is sensitive to the basic feature of the rule, which states that processes with disconnected quark lines between initial and final states are suppressed compared to those where the incident quarks continue through to the exit channel. The  $p + p$  collisions at RHIC are at an energy which is  $\sim 25$  times higher than energies where violations of the OZI rule were reported [33,34]. The  $\phi$  meson enhancement in heavy-ion collisions shows an increasing trend with centrality (Fig. 5). From this, we conclude that the observed enhancement of  $\phi$  production in heavy-ion collisions may not be due to OZI suppression of  $\phi$  production in  $p + p$  collisions.

The observed enhancement of  $\phi$  meson production then is a clear indication for the formation of a dense partonic medium being responsible for the strangeness enhancement in Au + Au collisions at 200 GeV. Furthermore,  $\phi$  mesons do not follow the strange quark ordering as expected in the canonical picture for the production of other strange hadrons [39]. The observed enhancement in  $\phi$  meson production being related to medium density is further supported by the energy dependence shown in the lower panel of Fig. 5. The  $\phi$  meson production relative to  $p + p$  collisions is larger at higher beam energy, a trend opposite to that predicted in canonical models for other strange hadrons. Earlier

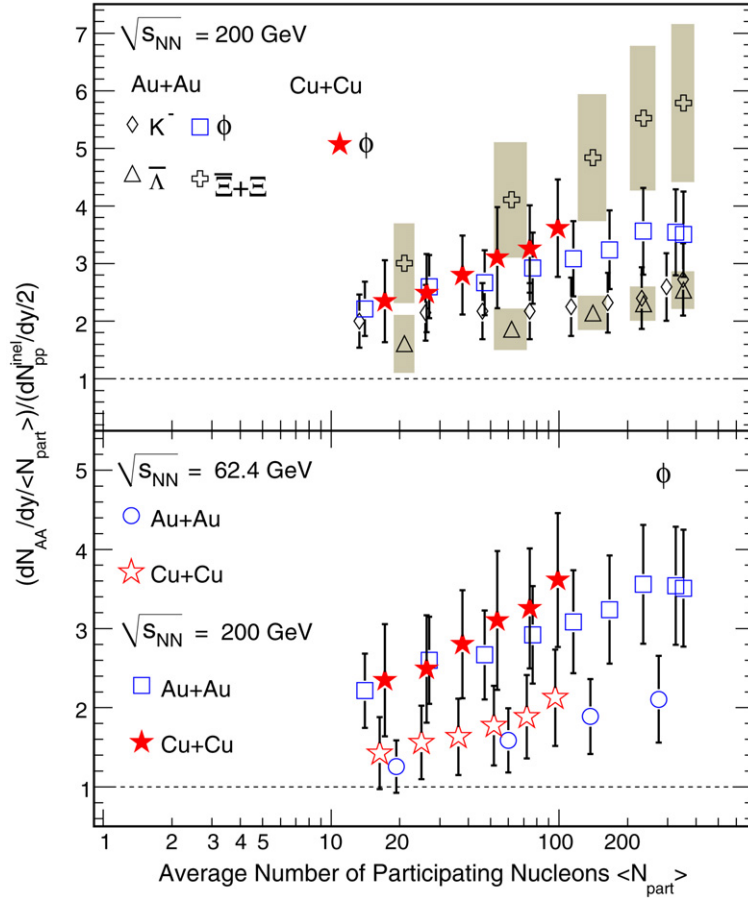


**Fig. 5.** Upper panel: The ratio of the yields of  $K^-$ ,  $\phi$ ,  $\bar{\Lambda}$  and  $\Xi + \bar{\Xi}$  normalized to  $\langle N_{\text{part}} \rangle$  in nucleus–nucleus collisions to corresponding yields in inelastic  $p + p$  collisions as a function of  $\langle N_{\text{part}} \rangle$  at 200 GeV. Lower panel: Same as above for  $\phi$  mesons in Cu + Cu collisions at 200 and 62.4 GeV. The  $p + p$  collision data at 200 GeV are from STAR [5] and at 62.4 GeV from ISR [29]. The error bars shown represent the statistical and systematic errors added in quadrature.

measurements have indicated that  $\phi$  meson production is not from the coalescence of  $K\bar{K}$  and is minimally affected by re-scattering effects in the medium [5]. Recent measurements indicate that  $\phi$  mesons are formed from the coalescence of seemingly thermalized strange quarks [3]. All these observations put together along with the observed centrality and energy dependence of  $\phi$  meson production (shown in Fig. 5) indicate the formation of a dense partonic medium in heavy-ion collisions where strange quark production is enhanced (possible mechanisms could be as discussed in Refs. [13,17]). This in turn suggests that the observed centrality dependence of the enhancement for other strange hadrons (shown in Fig. 5) is likely to be related to the same reasons as in the case of the  $\phi$  meson, that it is due to the formation of a dense partonic medium in the collisions. These experimental data rule out the possibility of canonical suppression being the only source of the observed strangeness enhancement at beam energies of 200 GeV. It may be mentioned that an enhancement factor of  $3.0 \pm 0.7$  was reported for  $\phi$ -mesons at top the SPS energy [10]. A study of energy dependence ( $\sqrt{s_{\text{NN}}} = 6\text{--}17$  GeV) of  $\phi$  meson production at SPS through central Pb + Pb collisions showed that at highest energies hadronic models fails to explain the data. A statistical hadron gas model with undersaturation of strangeness provided a better description of the measured  $\phi$  yields. This suggested that strangeness content at chemical freeze-out near top SPS energies could already have been determined on a partonic level [10].

## 6. Summary

We have presented a study of the energy and system size dependence of  $\phi$  meson production using the  $p + p$ , Cu + Cu and

Au + Au data at  $\sqrt{s_{\text{NN}}} = 62.4$  and 200 GeV. The  $p_{\text{T}}$  spectra are measured at midrapidity ( $|y| < 0.5$ ) over the range  $0.4 < p_{\text{T}} < 5$  GeV/c. These measurements provide new experimental results showing that at a given beam energy the transverse momentum spectra in both shape ( $\langle p_{\text{T}} \rangle$ ) and yields ( $dN/dy$ ) are similar in Cu + Cu and Au + Au for collisions with similar  $\langle N_{\text{part}} \rangle$ . In addition to observing similarity in the  $\phi$  meson distributions for Cu + Cu and Au + Au collisions with similar  $\langle N_{\text{part}} \rangle$ , the  $\langle N_{\text{part}} \rangle$  scaled nuclear modification factors are observed to be similar for the 0–10% central Cu + Cu and Au + Au collisions at 200 GeV. However, such a similarity is not seen for other collision centralities. The corresponding results for the nuclear modification factor, scaled by the number of binary collisions, are in general found to be higher for Cu + Cu compared to Au + Au collisions.

The enhancement in the  $\phi$  meson production has been studied through the ratio of the yields normalized to  $\langle N_{\text{part}} \rangle$  in nucleus–nucleus collisions to corresponding yields in  $p + p$  collisions as a function of  $\langle N_{\text{part}} \rangle$ . The centrality and energy dependence of the enhancement in  $\phi$  meson production clearly reflects the enhanced production of  $s$ -quarks in a dense medium formed in high energy heavy-ion collisions. This then indicates that the observed enhancements in other strange hadron ( $K^-$ ,  $\bar{\Lambda}$  and  $\Xi + \bar{\Xi}$ ) production in the same collision system are likely to be due to the similar effects and not only due to canonical suppression of strangeness production. At RHIC the colliding beam energy is high, so it is very unlikely that the observed enhancement in heavy-ion collisions is due to OZI suppression of  $\phi$  production in  $p + p$  collisions.

The enhancement in the  $\phi$  meson production deviates from the number of valence  $s$ -quark dependence observed for other strange hadrons. The results from  $\phi$  mesons lie in between those from



single valence  $s$ -quark carrying hadrons  $K^-$  and  $\bar{\Lambda}$ , and double valence  $s$ -quark carrying hadrons  $\Xi + \bar{\Xi}$ . Comparisons with other strange hadrons rule out the possibility of this being a baryon-meson or mass effect. The exact reason for the observed deviation of the enhancement factor for the  $\phi$  meson from the valence strange quark dependence observed for other strange hadrons is not fully clear. It could be due to the effect of light-flavor valence quarks in the other strange hadrons or due to the net strangeness being zero in  $\phi$  mesons. The other possibility is based on a recent theoretical work which decouples the system in heavy-ion collisions into a high density part (core) and a low density part (corona) are able to explain the enhancement and colliding system size dependence of  $\phi$ -meson production at RHIC [28].

### Acknowledgements

We thank the RHIC Operations Group and RCF at BNL, and the NERSC Center at LBNL and the resources provided by the Open Science Grid consortium for their support. This work was supported in part by the Offices of NP and HEP within the US DOE Office of Science, the US NSF, the Sloan Foundation, the DFG Excellence Cluster EXC153 of Germany, CNRS/IN2P3, RA, RPL, and EMN of France, STFC and EPSRC of the United Kingdom, FAPESP of Brazil, the Russian Ministry of Sci. and Tech., the NNSFC, CAS, MoST, and MoE of China, IRP and GA of the Czech Republic, FOM of the Netherlands, DAE, DST, and CSIR of the Government of India, Swiss NSF, the Polish State Committee for Scientific Research, and the Korea Sci. & Eng. Foundation.

### References

- [1] I. Arsene, et al., BRAHMS Collaboration, Nucl. Phys. A 757 (2005) 1; B.B. Back, et al., PHOBOS Collaboration, Nucl. Phys. A 757 (2005) 28; J. Adams, et al., STAR Collaboration, Nucl. Phys. A 757 (2005) 102; K. Adcox, et al., PHENIX Collaboration, Nucl. Phys. A 757 (2005) 184.
- [2] E.V. Shuryak, Phys. Rep. 61 (1980) 71.
- [3] B.I. Abelev, et al., STAR Collaboration, Phys. Rev. Lett. 99 (2007) 112301.
- [4] S. Afanasiev, et al., PHENIX Collaboration, Phys. Rev. Lett. 99 (2007) 112301.
- [5] J. Adams, et al., STAR Collaboration, Phys. Lett. B 612 (2005) 181.
- [6] S.S. Adler, et al., PHENIX Collaboration, Phys. Rev. C 69 (2004) 034909.
- [7] M. Bleicher, et al., J. Phys. G 25 (1999) 1859; Y. Cheng, et al., Phys. Rev. C 68 (2003) 034910.
- [8] A. Sibirtsev, et al., Eur. Phys. J. A 29 (2006) 209; A. Sibirtsev, et al., Eur. Phys. J. A 37 (2008) 287.
- [9] R.J. Fries, et al., Phys. Rev. C 68 (2003) 044902; L.-W. Chen, C.M. Ko, Phys. Rev. C 73 (2006) 044903; R.C. Hwa, C.B. Yang, Phys. Rev. C 75 (2007) 054904.
- [10] C. Alt, et al., NA49 Collaboration, Phys. Rev. Lett. 94 (2005) 052301; C. Alt, et al., NA49 Collaboration, Phys. Rev. C 78 (2008) 044907; C. Höhne, et al., Nucl. Phys. A 715 (2003) 474; D. Adamova, et al., CERES Collaboration, Phys. Rev. Lett. 96 (2006) 152301; S. Afanasiev, et al., NA49 Collaboration, Phys. Lett. B 491 (2000) 59.
- [11] L. Ahle, et al., E-802 Collaboration, Phys. Rev. C 60 (1999) 044904.
- [12] K.H. Ackermann, et al., Nucl. Instrum. Methods Phys. Res., Sect. A 499 (2003) 624.
- [13] A. Shor, Phys. Rev. Lett. 54 (1985) 1122.
- [14] A.J. Baltz, C. Dover, Phys. Rev. C 53 (1996) 362.
- [15] M. Berenguer, H. Sorge, W. Greiner, Phys. Lett. B 332 (1994) 15.
- [16] S. Okubo, Phys. Lett. 5 (1963) 165; G. Zweig, CERN Report Nos. TH-401 and TH-412 (1964) (unpublished); J. Iizuka, K. Okada, O. Shito, Prog. Theor. Phys. 35 (1966) 1061.
- [17] J. Rafelski, B. Muller, Phys. Rev. Lett. 48 (1982) 1066; P. Koch, B. Muller, J. Rafelski, Phys. Rep. 142 (1986) 167.
- [18] J. Cleymans, A. Muronga, Phys. Lett. B 388 (1996) 5; J. Cleymans, M. Marais, E. Suhonen, Phys. Rev. C 56 (1997) 2747.
- [19] J. Cleymans, et al., Phys. Rev. C 57 (1998) 3319; S. Hamieh, K. Redlich, A. Tounsi, Phys. Lett. B 486 (2000) 61.
- [20] K. Redlich, A. Tounsi, Eur. Phys. J. C 24 (2002) 589; A. Tounsi, K. Redlich, hep-ph/0111159.
- [21] J. Adams, et al., STAR Collaboration, Phys. Rev. Lett. 98 (2007) 062301; B.I. Abelev, et al., Phys. Rev. C 77 (2008) 044908.
- [22] M. Anderson, et al., Nucl. Instrum. Methods Phys. Res., Sect. A 499 (2003) 659.
- [23] J. Adams, et al., STAR Collaboration, Phys. Rev. C 73 (2006) 034906.
- [24] E. Yamamoto, PhD Thesis 2001, University of California, Los Angeles; J. Ma, PhD Thesis 2006, University of California, Los Angeles; S.-L. Blyth, PhD Thesis 2007, University of Capetown, Capetown; J. Chen, PhD Thesis, Shanghai Institute of Applied Physics, CAS (2008), unpublished; <http://drupal.star.bnl.gov/STAR/theses>.
- [25] S. Eidelman, et al., Particle Data Group, Phys. Lett. B 592 (2004) 39.
- [26] B.I. Abelev, et al., STAR Collaboration, arXiv:0809.4737.
- [27] P. Nevski, in: Proceedings of International Conference on Computing in High Energy and Nuclear Physics, Padova, Italy, 2000.
- [28] J. Aichelin, K. Werner, arXiv:0810.4465; F. Becattini, J. Manninen, arXiv:0811.376.
- [29] T. Akesson, et al., AFS Collaboration, Nucl. Phys. B 203 (1982) 27.
- [30] B.I. Abelev, et al., STAR Collaboration, Phys. Lett. B 655 (2007) 104; B.I. Abelev, et al., Phys. Rev. Lett. 97 (2006) 152301; B. Mohanty, for STAR Collaboration, nucl-ex/0705.0953.
- [31] C. Adler, et al., STAR Collaboration, Phys. Rev. Lett. 87 (2001) 182301.
- [32] R.A. Donald, et al., Phys. Lett. B 61 (1976) 210.
- [33] V. Blobel, et al., Phys. Lett. B 59 (1975) 88.
- [34] A. Sibirtsev, J. Haidenbauer, U.-G. Meissner, Eur. Phys. J. A 27 (2006) 263.
- [35] C.W. Akerlof, et al., Phys. Rev. Lett. 39 (1977) 861.
- [36] C. Daum, et al., ACCMOR Collaboration, Phys. Lett. B 98 (1981) 313.
- [37] M. Hartmann, et al., Phys. Rev. Lett. 96 (2006) 242301; M. Abdel-Bary, et al., COSY-TOF Collaboration, Phys. Lett. B 647 (2007) 351.
- [38] H.J. Lipkin, Phys. Lett. B 60 (1976) 371; J. Ellis, et al., Phys. Lett. B 353 (1995) 319.
- [39] I. Kraus, et al., Phys. Rev. C 76 (2007) 064903.